# Modelling of the IR Intensity Maps for HAEBE Stars with Algol-like Minima

Vladimir Il'in[1], Natalia Krivova[2] and Alexander Men'shchikov[1]

[1] Max Planck Society, Research Unit "Dust in Star-Forming Regions", Schillergäßchen 3, D-07745 Jena, Germany
[2] Astronomical Institute, St. Petersburg University, 198904 St. Petersburg, Russia

**Abstract.** A numerical radiative transfer code is used to compute intensity maps of the circumstellar dust shells around the HAEBE stars with Algol-like minima in spectral region from near to far infrared. Parameters of the shell models were determined from fitting of infrared spectra, colour–magnitude diagrams and circumstellar extinction curves. Main features of the shell images are discussed and their dependence on the model parameters is considered.

## 1 Introduction

While it is well known that Herbig Ae/Be (HAEBE) stars are surrounded by gas and dust, our understanding of these dusty shells still remains incomplete. The shell models are based on observed spectral energy distributions in infrared (IR), "circumstellar" (CS) extinction curves in ultraviolet (UV) and, for HAEBE stars with Algol-like minima (UX Ori, WW Vul, etc.), on colour–magnitude diagrams showing a "blueing" effect.

We refrain from commonly used method of fitting of one kind of the observational data only (usually IR spectra), since such an approach does not allow one to constrain even the parameters of the simplest models (see, e.g., Thamm et al. 1994; Men'shchikov & Henning 1995a). We believe that only a fitting of all the data may give a confidence in the derived values of the parameters.

During several last years, images of the shells around brightest HAEBE stars have been obtained at different wavelenghts from visual to far IR (see, e.g., Nakajima & Golimowski 1995; Di Francesco et al. 1994). In this paper, we briefly discuss whether these data could be used to constrain the shell parameters.

## 2 Model

To reduce a large number of free parameters we adopt the following simple model: the star is surrounded by a spherical shell with an optical thickness $\tau_V < 1$, power law density distribution $\rho(r) \sim r^{-\alpha}$, and minimum and maximum radii $R_{in}$ and $R_{out}$, respectively. The dust grain model used is a usual MRN-like one: a mixture of silicate and graphite grains having a power-law size distribution $n(a) \sim a^{-q}$ with the minimum and maximum sizes $a_{min}$ and $a_{max}$. A simple power-law $\rho(r)$

and the same sizes of silicate and graphite grains for the whole shell are justified by the absence of any detailed observational constraints.

Since the stellar parameters are usually well determined, our model has eight parameters: $\tau_V$, $\alpha$, $R_{in}$, $R_{out}$, and $n_{si}/n_{gr}$, $q$, $a_{min}$, $a_{max}$. Fitting of IR spectrum can constrain $\alpha, \tau_V, R_{in}$; colour–magnitude diagrams help to estimate $\tau_\lambda$ and $\Lambda_\lambda$, albedo of grains (see Krivova & Il'in 1995). Extinction curves in UV can give information on $a_{min}$, $q$, $n_{si}/n_{gr}$, but at the moment only for one HAEBE star with Algol-like minima these data are available.

For our modelling we used the radiative transfer method and the code described by Men'shchikov & Henning (1995b). The method is usable in both spherical and disk geometry with an arbitrary number and distribution of dust grain components (chemical composition, sizes).

## 3 Results

We have computed intensity maps of the shells at different wavelengths from visual to far IR, using the values of the model parameters derived by fitting IR spectra and colour–magnitude diagrams (see Krivova & Il'in 1995).

Figure 1 gives the distribution of specific intensity $I_\nu$ vs. impact parameter $b$. It is easy to follow the change of the distributions with wavelength. At $\lambda \approx 0.6$–$1.25$ $\mu m$, we have $I_\nu(b) \sim b^{-(1+\alpha)}$ in agreement with a simple theoretical model of the shell with a density gradient and single scattering (see, e.g., Weintraub et al. 1992); at $\lambda \sim 3$ $\mu m$ only very hot grains in the inner layers are seen; at $\lambda \sim 10$–$20$ $\mu m$ the intensity distribution becomes wider and for $\lambda > 60$ $\mu m$ the radiation comes from the whole shell.

Figure 2 shows the size of image area which produces half of the total flux at a given wavelength. The transition from scattered light to the thermal emission of dust at 2–3 $\mu m$ is clearly seen. To observe the shells at shorter wavelengths one needs to use coronographic techniques (or lunar occultations).

Let us now consider how the maps change with variations of the model parameters. We selected the following characteristics of the maps: ($i$) surface brightness in the R and I bands ($I_R, I_I$) at distance of 5000 AU (12$''$ at D=400pc) from a star and ($ii$) sizes of the shell projection which gives half of the total flux at 3, 10, 25 and 100 $\mu m$ ($R_3, R_{10}, R_{25}$ and $R_{100}$).

We varied the model parameters, keeping $\tau_V$ constant since it is relatively well constrained by observational data, and found that:
- $I_{R,I}$ and $R_\lambda$ for $\lambda > 10\mu m$ strongly depend on $\alpha$;
- $I_{R,I}$ and $R_\lambda$ for $\lambda < 8\mu m$ change with $a_{min}$ and $q$;
- $\tau_V$ affects only $I_{R,I}$ ($I \sim \tau\Lambda$);
- $R_{in}$ is important only for $R_\lambda$ with $\lambda < 15\mu m$;
- neither $I_{R,I}$ nor $R_{3,10,25,100}$ depend on $R_{out}$ and $a_{max}$.

Thus, from the intensity maps in the R and I bands one may expect to constrain $\alpha$ (and possibly $a_{min}$ and $q$); while from the far IR scans/maps and from the near IR observations with very high angular resolution - $\alpha$ and $R_{in}$ (and $a_{min}$, $q$), respectively.

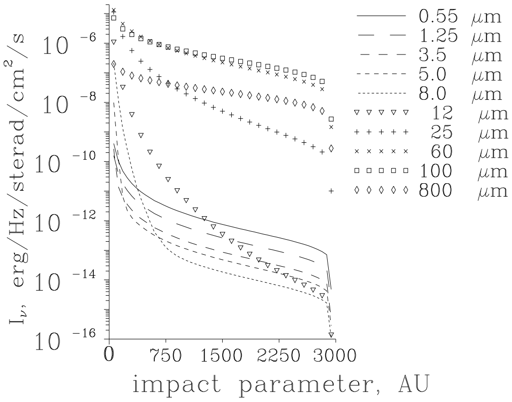


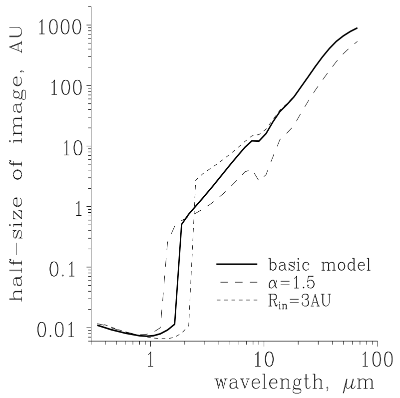


**Fig. 1.** The distribution of specific intensity vs. impact parameter. The model used — $T_{eff} = 8000$K, $L = 25 L_\odot$, $D = 250$pc, $R_{in} = 1$AU, $R_{out} = 3000$AU, $\alpha = 1.0$, $\tau_V = 0.9$, $a_{min} = 0.007\mu m$, $a_{max} = 0.25\mu m$, $q = 4.0$

**Fig. 2.** The size of image area producing half of the total flux at given wavelength. For basic model parameters see Fig. 1.

## 4 Example of AB Aur

The shells around UX Ori-like stars practically were not mapped so far. High resolution observations have been made only for brighter HAEBE stars without Algol-like minima, for example, AB Aur. As an illustration, we compare available observational images of this star with theoretical maps. For AB Aur we adopt Sorrell's (1990) model which gives a good fit to the observed IR spectrum and extinction curve (for $\lambda > 0.16\mu m$): $\tau_V = 0.05, \alpha = -1.0, R_{in} = 0.2AU, R_{out} = 20000AU, q = -3.5, n_{si}/n_{gr} = 0.6, a_{min} = 0.005\mu m$, $a_{max} = 1.0\mu m$.

Four works presenting observations of the vicinity of AB Aur with a high angular resolution were found in the literature:
- scans of AB Aur environment at $\lambda$ 100 $\mu m$ made by Di Francesco et al. (1994) have shown FWHM to be $< 14''$ (or <2000AU);
- at $\lambda$ 11.7 and 17.9 $\mu m$ the shell of AB Aur was observed at the 5-m telescope by Marsh et al. (1994) with FWHM of about 40 and 80AU, respectively;
- speckle-interferometry in the K band with resolution of $0.03''$ (5 AU) made by Leinert et al. (1994) gave no way to resolve the shell;
- coronographic images in the R and I bands obtained by Nakajima & Golimowski (1995) have shown a non-spherical matter distribution with the brightness of about 20 mag/$\square''$ at distances 10–$20''$ from the star.

Our calculations show that Sorrell's model gives $R_{100} = 5000$AU, $R_{20} = 70$AU, $R_{11} = 20$AU, $R_{2.2} < 0.01$AU, and $I_{I,R} \sim 13$ mag/$\square''$ at distance $\sim 15''$. The difference between the observed and theoretical values would be much smaller if we selected steeper density distribution ($\alpha = -1.5$). However, we do not consider this model in more detail because its inner radius is certainly wrong. At the distance of 0.2AU from the star grains would have temperature higher than 2500K, i.e. they cannot exist there.

The HAEBE stars with Algol-like minima for which our model was developed are at least 2.5 times more distant than AB Aur (D=160pc for the latter). At the moment it seems impossible to resolve their shells at 10 or 100 $\mu m$, but faint ($\sim$ 21 mag/$\square''$) reflection nebulae could be detected by coronographic techniques.

## 5 Conclusions

We have computed intensity maps for simple shell models giving the observed spectral energy distributions and colour–magnitude diagrams for HAEBE stars with Algol-like minima. We have considered the main features of the shell images and their dependence on the model parameters. We found clear relationships between surface brightness distributions and some of the parameters. Thus, the shell images, providing important information on geometry of the shells, could give new constraints on their physical parameters (but only when being considered together with other observational data!).

As a next step we are going to model existing polarization data as well, using a spheroidal model of the shells and a Monte-Carlo code (Fischer et al. 1994). This must add one model parameter, the shell semiaxes ratio, but would allow one to involve more data into consideration: total polarization of the objects at different wavelengths and polarization maps of scattered light. We should mention that with the polarization data we shall be abble to involve into consideration all the data available for our stars.

**Acknowledgments.** We thank Dr. B. Stecklum for comments. V. I. acknowledges the support from the Alexander von Humboldt Foundation. N. K. thanks the Government of St. Petersburg for the financial support (Young Scientists Program grant 138-2-2.2).

## References

Di Francesco, J., Evans II, N. J., Harvey, P. M., Mundy, L. G., Butner, H. M. (1994): ApJ **432**, 710–719

Fischer, O., Henning, Th., Yorke, H. W. (1994): A&A **284**, 187–209

Krivova, N. A., Il'in, V. B., (1995): This volume

Leinert, Ch., Richichi, A., Weitzel, N., Haas, M. (1994): eds. Thé, P. S., Perez, M. R., van den Heuvel, E. P. J. "The nature and evol. status of HAEBE stars", p. 155

Marsh, K. A., van Cleve, J. E., Mahoney, M. J., Hayward, T. L., Houck, J. R. (1994): BAAS **26**, 931

Men'shchikov, A. B., Henning, Th. (1995a): This volume

Men'shchikov, A. B., Henning, Th. (1995b): A&A (submitted)

Nakajima, T., Golimowski, D. A. (1995): AJ **109**, 1181–1198

Prusti, T., Natta, A., Palla, F. (1994): A&A **292**, 593–598

Thamm, E., Steinacker, J., Henning, Th. (1994): A&A **287**, 493–502

Weintraub, D. A., Kastner, J. H., Zuckerman, B., Gatley, I. (1992): ApJ **391**, 784–804